Leptogenesis with a dynamical seesaw scale

D. Aristizabal Sierra,[1,*] M. Tórtola,[2,†] J. W. F. Valle,[2,‡] and A. Vicente[1,§]

[1] *IFPA, Dep. AGO, Universite de Liege, Bat B5, Sart Tilman B-4000 Liege 1, Belgium*

[2] *AHEP Group, Institut de Física Corpuscular – C.S.I.C./Universitat de València, Parc Cientific de Paterna. C/ Catedratico Jose Beltran, 2 E-46980 Paterna (València) - SPAIN*

(Dated: July 2, 2014)

In the simplest type-I seesaw leptogenesis scenario right-handed neutrino annihilation processes are absent. However, in the presence of new interactions these processes are possible and can affect the resulting $B-L$ asymmetry in an important way. A prominent example is provided by models with spontaneous lepton number violation, where the existence of new dynamical degrees of freedom can play a crucial role. In this context, we provide a model-independent discussion of the effects of right-handed neutrino annihilations. We show that in the weak washout regime, as long as the scattering processes remain slow compared with the Hubble expansion rate throughout the relevant temperature range, the efficiency can be largely enhanced, reaching in some cases maximal values. Moreover, the $B-L$ asymmetry yield turns out to be independent upon initial conditions, in contrast to the "standard" case. On the other hand, when the annihilation processes are fast, the right-handed neutrino distribution tends to a thermal one down to low temperatures, implying a drastic suppression of the efficiency which in some cases can render the $B-L$ generation mechanism inoperative.

PACS numbers: 13.35.Hb, 13.15.+g, 14.60.Pq, 14.60.St, 11.30.Fs

I. INTRODUCTION

The only indications for physics beyond the $\mathrm{SU(2)_L \otimes U(1)_Y}$ model come from the lepton sector and cosmology. In particular, the need to account for neutrino mass [1] as well as the cosmological baryon asymmetry [2, 3] have brought substantial interest on different variants of the seesaw mechanism with high [4–9] as well as low lepton number violation scale [10–13]. Like the electroweak gauge symmetry, it is reasonable to imagine that also lepton number symmetry is broken spontaneously in order to generate neutrino masses. A simple framework for this is the $\mathrm{SU(2)_L \otimes U(1)_Y}$ seesaw scenario with spontaneous violation of ungauged lepton number [14–17], whose implementation requires the presence of a lepton-number-carrying complex scalar singlet coupled to the electroweak singlet right-handed (RH) neutrinos. Its imaginary part is the associated Nambu-Goldstone boson which could pick up mass in the presence of small terms in the scalar potential with explicit lepton number violation that might arise, say, from quantum gravity effects [18]. Apart from its intrinsic interest as an attractive neutrino mass generation scheme, it has been suggested that, the resulting Nambu-Goldstone boson could play an interesting role in cosmology, either providing a viable dark matter candidate [19–22], or bringing in the CP-even physical degree of freedom the state responsible for driving

*Electronic address: daristizabal@ulg.ac.be
†Electronic address: mariam@ific.uv.es
‡Electronic address: valle@ific.uv.es
§Electronic address: Avelino.Vicente@ulg.ac.be

inflation [23, 24], as hinted by recent cosmological data [25].

Besides providing a compelling framework for neutrino masses and mixings, with all its phenomenological features, such majoron scenario involves new ingredients which can affect the generation of the $B-L$ asymmetry. Let us discuss this in more detail. In type-I seesaw with explicit lepton number violation, a nonzero $B-L$ asymmetry is generated by the out-of-thermal-equilibrium and CP violating decays of the lightest right-handed neutrino [26–28]. This $B-L$ asymmetry is then partially reprocessed into a baryon asymmetry by standard model electroweak sphaleron processes [29], thus providing an explanation for the origin of the cosmic baryon asymmetry. In this framework the RH neutrinos only have Yukawa interactions, which are responsible for a non-vanishing RH neutrino distribution as well as for the crucial $B-L$ washout processes. This picture is to some extent oversimplified and can dramatically change whenever the RH neutrinos possess additional interactions beyond those of the simplest type-I seesaw scenario. This is indeed what happens in seesaw models with spontaneous lepton number breaking in which RH neutrino masses rather than being put in "by hand", arise via a dynamical mechanism, similar to the breaking of the standard model gauge symmetry.

In this paper we study the effects induced by these new right-handed neutrino couplings upon the RH neutrino distribution, which ultimately affect the resulting $B-L$ asymmetry. While similar considerations apply also to theories of gauged lepton number, such as models with a local U(1) lepton number symmetry [30], Pati-Salam [31], left-right symmetric [8], here we focus upon the simplest $\mathrm{SU(3)_c}\otimes\mathrm{SU(2)_L}\otimes\mathrm{U(1)_Y}$ scheme based upon spontaneously broken ungauged lepton number [14, 15]. In addition to the standard model fields and three RH neutrinos, the simplest of such seesaw models involves also a complex $\mathrm{SU(3)_c}\otimes\mathrm{SU(2)_L}\otimes\mathrm{U(1)_Y}$ singlet scalar carrying two units of lepton number, denoted by σ. The relevant invariant Yukawa interactions are

$$-\mathcal{L}_Y = \bar{N}_\alpha\,\lambda_{\alpha i}\,\ell_i\,\tilde{H}^\dagger + \frac{1}{2}\,\bar{N}_\alpha\,C\,h_{\alpha\beta}\,\bar{N}^T_\beta\,\sigma + \mathrm{H.c.}\,, \tag{1}$$

where ℓ denotes the lepton doublet, λ is a general complex 3×3 matrix and h is a complex symmetric 3×3 matrix in generation space. The resulting seesaw scheme is characterized by singlet and doublet neutrino mass terms, described in matrix form as

$$\mathcal{M}_\nu = \begin{pmatrix} 0 & \lambda\,\langle H\rangle \\ \lambda^T\,\langle H\rangle & h\,\langle\sigma\rangle \end{pmatrix}. \tag{2}$$

Here $\langle H\rangle$ determines the masses of the weak gauge bosons, the $W^\pm$ and the Z^0, hence $\langle H\rangle = v/\sqrt{2}\simeq 174$ GeV, while the spontaneous lepton number violation occurs at the scale $\langle\sigma\rangle = u/\sqrt{2}$. This vacuum expectation value (vev) drives spontaneous lepton number violation and induces the RH Majorana neutrino mass matrix $M_N = h\,\langle\sigma\rangle$ together with residual Yukawa interactions from $NN\sigma$ in Eq. (1). The diagonalization of the neutrino mass matrix $\mathcal{M}_\nu$ proceeds through a unitary mixing matrix as $U^T\mathcal{M}_\nu U = \mathrm{diag}(m_i, M_i)$ [9], yielding 6 mass eigenstates, the three light neutrinos with masses $m_i\sim\lambda^2v^2/M_N$, and three heavy neutrinos. The gauge invariant tree-level Higgs scalar potential associated to the singlet and doublet scalar multiplets σ and H is a simple extension of that which characterizes the standard model and is given by

$$V(H,\sigma) = V_{\mathrm{SM}}(H) + V_{\mathrm{BSM}}(H,\sigma) = \lambda_H|H|^4 - m_H^2|H|^2 + \lambda_\sigma|\sigma|^4 - m_\sigma^2|\sigma|^2 + \delta|H|^2|\sigma|^2\,, \tag{3}$$

where the first two terms correspond to V_{SM} and the remaining ones account for either pure σ interactions or the singlet-doublet coupling. Note that cubic terms of the type $\sigma|H|^2$ or σ^3 are absent due to lepton number conservation. The full scalar potential V will be bounded from below as long as the conditions $\lambda_\sigma,\lambda_H>0$ and $\delta>-2\sqrt{\lambda_\sigma\lambda_H}$ are satisfied. After minimization, one finds, as expected, two physical CP-even scalar bosons and one CP-odd state, identified with the majoron J [14, 15], the Goldstone boson associated to the spontaneous breaking of lepton number.

It is clear that in such schemes there will be a number of new processes involving the new spin zero states which may have an impact on the way the $B-L$ generation mechanism proceeds. In particular, the RH neutrino Yukawa coupling

$N\,N\,\sigma$ will induce s,t,u-channel $2 \leftrightarrow 2$ scattering processes $N_1 N_1 \leftrightarrow h_i h_j$ and $N_1 N_1 \leftrightarrow JJ$. If the thermal bath is populated with the new scalars before the leptogenesis era [32], these processes can efficiently populate the plasma with RH neutrinos, basically resembling what happens in scalar and fermion triplet leptogenesis models [33–36]. If this turns out to be the case, soon after these processes become active the heat bath can be readily populated with a RH neutrino thermal distribution, thus implying that if at early times the $2 \leftrightarrow 2$ scattering processes and the RH neutrinos inverse decays are frozen, a sizeable enhancement of the $B-L$ yield can be expected. Moreover, with these $2 \leftrightarrow 2$ scattering processes being fast at early epochs, the $B-L$ asymmetry will be certainly independent upon initial conditions, even in the weak washout regime. On the other hand, if scatterings remain efficient till late epochs, the number of RH neutrinos available in the heat bath can drastically decrease, thus leading to an important depletion of the $B-L$ yield [37]. Our aim in this paper is to provide a quantitative analysis of all these effects, identifying the implications of these new reactions in the type-I seesaw leptogenesis picture. In particular we explore up to which extent the condition of successful leptogenesis constrains the parameters of these models. Before we proceed let us emphasize the generality of our study. Although motivated by type-I seesaw models with spontaneous lepton number violation, these effects in seesaw leptogenesis are not restricted to majoron models. In general, they will be present in all models with extended scalar sectors that couple to the RH neutrinos. These include all schemes with a $NN\sigma$ coupling, such as other variants of majoron models [16], flavon models, etc.

The rest of the paper is organized as follows: in Sec. II we establish the basic assumptions of our analysis (fulfilled by the lepton number violation model we are interested in) and present some general aspects of leptogenesis in models with extended scalar sectors. In Sec. III we show our general results, to be interpreted in the minimal majoron model in Sec. IV. Finally, we summarize our results and conclude in Sec. V.

II. GENERALITIES

All majoron schemes require an extended set of physical scalars. We now proceed to a more detailed and general study of the implications of having additional scalars in leptogenesis seesaw scenarios. The basic particle physics input is the CP asymmetry parameter ϵ_{N_1} characteristic of seesaw leptogenesis [26–28]. In order to determine the final $B-L$ asymmetry yield one must also take into account all $B-L$ production and washout processes. In general, the scalar sector gives rise to new contributions to these. For example, the new scalars could contribute to the CP asymmetry ϵ_{N_1} as well as provide new source/washout terms in the kinetic equations, potentially affecting the constraints on the $B-L$ generation scale [38]. However, we neglect such possible contributions and focus on the role of the RH neutrino scatterings, assuming the following conditions:

(A) In addition to the usual type-I seesaw Lagrangian (in the basis where the RH neutrino mass matrix is diagonal) [1]

$$\mathcal{L}_{\rm seesaw} = \bar{N}_\alpha\, \lambda_{\alpha i}\, \ell_i\, \tilde{H}^\dagger + \frac{1}{2} \bar{N}_\alpha\, C\, M_{N_{\alpha\alpha}}\, \bar{N}_\alpha^T + \text{H.c.}\ , \tag{4}$$

there are new interactions generically described by the following terms

$$\mathcal{L} \supset \frac{1}{2} g_{N_\alpha N_\beta a}\, \bar{N}_\alpha\, C\, \bar{N}_\beta^T\, S_a + \mu_{abc}\, S_a\, S_b\, S_c\ + \text{H.c.} \tag{5}$$

The dimensionless coupling $g_{N_\alpha N_\beta a}$ and the mass parameters μ_{abc} characterize the scalar sector as arising, for example, in the type-I seesaw majoron scheme. Here the S_a's correspond to mass eigenstates.

---

[1] We choose to denote RH neutrino generations with Greek letters $\alpha, \beta, \gamma, \ldots$, lepton flavors with the Latin letters $i, j, k, \ldots$, while the extra scalars are labeled with the Latin letters $a, b, c, \ldots$.

(*B*) All the CP violating phases involved in the generation of a non-vanishing $B-L$ asymmetry are entirely attached to the Dirac Yukawa couplings.

Under these assumptions the leading $\mathcal{O}(\lambda^2)$ reactions relevant for the generation of the $B-L$ asymmetry include the following processes: $\Delta L=1$ decay and inverse decay reactions $N_1 \leftrightarrow \ell\, H$; s-channel off-shell $\Delta L=2$ scatterings $H\,\ell \leftrightarrow H\,\ell$ and s,t,u-channel $N_1 N_1 \leftrightarrow S_a\, S_b$ scatterings implied by Eq. (5). The new $2\leftrightarrow 2$ scattering reactions resemble those found in type-II or type-III seesaw leptogenesis scenarios, where the states responsible for the generation of the $B-L$ asymmetry–having non-trivial electroweak charges–possess vector-boson-mediated annihilations [33–36, 39, 40]. These reactions are also present when RH neutrinos have non-trivial gauge charges, as in left-right symmetric models [41–43] or models with additional $U(1)$ gauge groups [44–47]. However, compared with majoron models these scenarios differ in several aspects. For example: (*i*) in some cases the resulting $B-L$ asymmetry can be a combination of non-thermal and thermal contributions [47]; (*ii*) the gauge scattering processes, although present, are of no relevance [43]. Furthermore, there is a fundamental difference: while the vector-boson-mediated annihilations at high temperatures are always fast (their rate is faster then the Universe Hubble expansion rate), the RH neutrino annihilations in majoron models are controlled by free parameters. Depending on the size of the couplings in Eq. (5) and on the RH neutrino mass, these scattering reactions may have new effects. First, if after reheating, the heat bath turns out to be populated with the new scalars (in addition to the standard model particles) [32], the $2\leftrightarrow 2$ scatterings could populate the plasma with RH neutrinos in addition to those coming from RH neutrino inverse decays. On the other hand, for sufficiently fast scattering processes the resulting $B-L$ asymmetry will no longer depend upon initial conditions, even if the asymmetry is generated within the weak washout regime. Moreover, fast $2\leftrightarrow 2$ processes will tend to thermalize the RH neutrino distribution. This implies that the generation of the $B-L$ asymmetry will no longer be determined solely by reactions involving the Dirac Yukawa couplings λ but instead by an interplay between decays and RH neutrino annihilations.

Rather than demanding the scalar-mediated RH neutrino annihilations to be slow, $\gamma_S/n_N^{\rm Eq}\,H \lesssim 1$ (γ_S being the annihilation reaction density), what really matters is the relative size between the decay and annihilation reaction densities. Thus, one can distinguish two types of scenarios, those for which $\gamma_S \ll \gamma_D$, γ_D denoting the decay reaction density, and those for which the annihilation processes are fast and satisfy $\gamma_S > \gamma_D$ during certain range in $z=M_{N_1}/T$. In the former case the annihilation reactions are negligible and the generation of the $B-L$ asymmetry proceeds in the standard way. On the other hand in the latter case a sizeable $B-L$ asymmetry requires decays and scatterings to become slow.

In order to illustrate the general features of these scenarios one must calculate the annihilation reaction density, and this requires specifying the number of scalar degrees of freedom participating in the annihilation process. For definiteness, here we assume that the extended scalar sector contains three new scalars S_1, S_2 and S_3 of which $S_{1,2}$ are CP even states and S_3 is a CP odd field. This pattern arises in the simplest majoron scheme, in which case S_3 would correspond to the majoron. When combined with assumption B, these CP transformation properties imply the absence of interactions with an odd power in S_3, such as $N_\alpha\, N_\alpha\, S_3$ and $S_a\, S_b\, S_3$. Thus, the presence of these new scalar states induces the scattering processes $N_1\, N_1 \to S_a\, S_a$ [2] determined by s-channel $S_{1,2}$ exchange and t- and u-channel N_1-mediated processes [3], as shown in Fig. 1. As a function of the annihilation center-of-mass energy $\sqrt{s}$, the cross section for the $N_1\, N_1 \to S_a S_a$ scattering processes is then given by four terms, namely

$$\sigma(N_1\, N_1 \to S_a\, S_a) \equiv \sigma_S^{(a)}(s) = \sigma_s^a(s) + \sigma^{(a)}_{s_1(t,u)}(s) + \sigma^{(a)}_{s_2(t,u)}(s) + \sigma^{(a)}_{(t,u)}(s)\ , \tag{6}$$

---

[2] Strictly speaking, in addition to CP conservation, we are also assuming that all RH neutrinos have the same CP parity [48, 49]. Moreover, for simplicity, we neglect off-diagonal scattering processes $N_1\, N_1 \to S_a\, S_b$, with $a \neq b$, as they would not add any essentially new feature.

[3] In principle one should also consider $N_{2,3}$-mediated processes. In order to reduce the number of free parameters we have neglected these contributions. This is well justified for strongly hierarchical RH neutrinos, where such contributions are sub-leading.

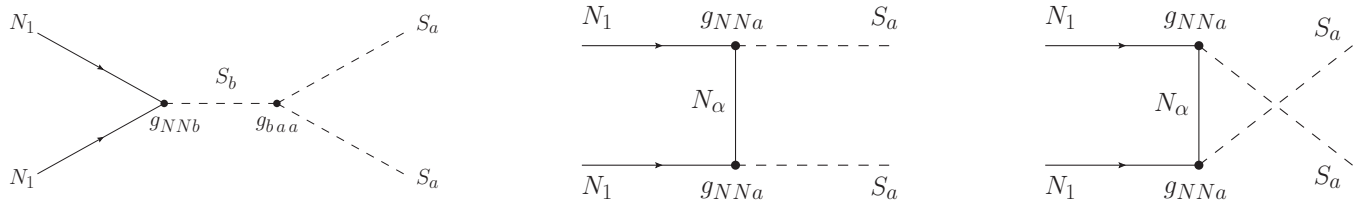

FIG. 1: *s-, t- and u-channel processes contributing to the total $N_1\,N_1 \to S_a\,S_a$ annihilation cross section. In our calculations we will only consider diagrams with $N_\alpha = N_1$ (see footnote 3).*

with the first term arising from the $S_{1,2}$ s-channel processes, the second and third terms from the interference between s-channel and t- and u-channel reactions, while the last term is due to t- and u-channel processes only. Explicitly, we have

$$\sigma_s^{(a)}(s) = \frac{1}{16\pi\, s}\frac{r_{S_a}}{r_N}\frac{\omega}{x_N}\left(\frac{g_{1aa}^2\, g_{NN1}^2}{\bar{r}_{S_1}^2} + 4\frac{g_{1aa}\, g_{2aa}\, g_{NN1}\, g_{NN2}}{\bar{r}_{S_1}\bar{r}_{S_2}} + \frac{g_{2aa}^2\, g_{NN2}^2}{\bar{r}_{S_2}^2}\right)\,, \tag{7}$$

$$\sigma^{(a)}_{s_{(1,2)}(t,u)}(s) = \frac{g_{NN(1,2)}\, g_{NNa}^2\, g_{(1,2)aa}}{4\pi\, s}\frac{1}{r_N^2\,\bar{r}_{S_{(1,2)}}}\frac{\omega}{x_N}\,\log\left[\frac{c_{Na}\, x_N(1-r_N\, r_{S_a})-2}{c_{Na}\, x_N(1+r_N\, r_{S_a})-2}\right]\,, \tag{8}$$

$$\begin{aligned}\sigma^{(a)}_{(t,u)}(s) = \frac{g_{NNa}^4}{2\,\pi\, s}\frac{r_{S_a}}{r_N}\,c_{Na}\,\omega\,\Bigg\{&\frac{c_{Na}\, x_N}{[c_{Na}\, x_N(1+r_N\, r_{S_a})-2]\,[c_{Na}\, x_N(1-r_N\, r_{S_a})-2]}\\ &+\frac{1}{2r_N\, r_{S_a}\,(c_{Na}\, x_N-2)}\log\left[\frac{c_{Na}\, x_N(1+r_N\, r_{S_a})-2}{c_{Na}\, x_N(1-r_N\, r_{S_a})-2}\right]\Bigg\}\,.\end{aligned} \tag{9}$$

In these expressions the following conventions have been adopted: $r_N = \sqrt{1-4/x_N}$, $r_{S_a} = \sqrt{1-(4/c_{Na}\, x_N)}$, $\bar{r}_{S_{1,2}} = 1-(1/c_{N(1,2)}\, x_N)$ and $\omega = 1-2/x_N$, with $x_N = s/M_{N_1}^2$ and $c_{Na} = M_{N_1}^2/m_{S_a}^2$. Moreover, we denote $g_{NNa} \equiv g_{N_1N_1a}$. Under our assumptions the left diagram can produce three scalars whereas the others only produce S_1 and S_2. We have also introduced the dimensionless parameter $g_{(1,2)aa} = \mu_{(1,2)aa}/M_{N_1}$. In the derivation of the cross section none of the scalar masses have been neglected, the vanishing scalar mass limit–applicable in a large variety of scenarios–corresponds to $c_{Na} \to \infty$. The total cross section is then given by

$$\sigma_S(s) = \sum_{a=1}^{3}\sigma_S^{(a)}(s)\,, \tag{10}$$

Using the expressions Eq. (7), (8) and (9) one can derive the reduced cross section, $\widehat{\sigma}(x_N) = 2s\,\sigma_S(s)\,r_N^2$, that enables the calculation of the $N_1\,N_1 \to S_a\,S_a$ reaction density:

$$\gamma_S = \frac{M_{N_1}^4}{64\,\pi^4}\int_4^\infty dx_N\,\sqrt{x_N}\,\frac{K_1(z\sqrt{x_N})}{z}\,\widehat{\sigma}_S(x_N)\,, \tag{11}$$

where $K_1(z)$ is a modified Bessel function. For the decay reaction density, instead, the following expression holds

$$\gamma_D = \frac{M_{N_1}^3}{\pi^2}\frac{K_1(z)}{z}\,\Gamma_{N_1}^{\rm Tot} \qquad \text{with} \qquad \Gamma_{N_1}^{\rm Tot} = \frac{M_{N_1}^2}{8\,\pi\, v^2}\,\widetilde{m}_1\,, \tag{12}$$

with v defined as in Sec. I, namely $\langle H\rangle = v/\sqrt{2} \simeq 174$ GeV, and the "effective" mass parameter $\widetilde{m}_1$, determined by the leading seesaw contribution to light neutrino masses,

$$\widetilde{m}_1 = \frac{v^2}{M_{N_1}}\left(\lambda\,\lambda^\dagger\right)_{11}\,. \tag{13}$$

With the setup of Eqs. (7)-(9), (11) and (12), the different scenarios one can consider can now be illustrated. In order to proceed one must specify a point in parameter space which consist of $\tilde{m}_1$, M_{N_1}, the scalar and RH neutrino mass

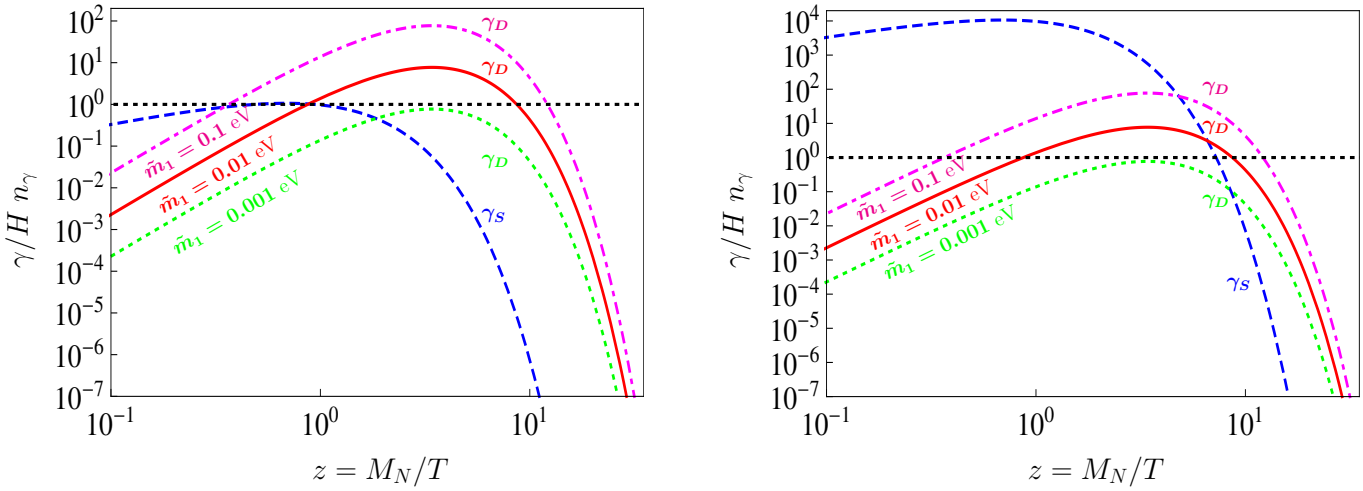

FIG. 2: Right-handed neutrino scalar-mediated annihilation and decay reaction densities as a function of $z = M_{N_1}/T$ for $M_{N_1} = 10^{10}$ GeV. In the left plot we have chosen $\bar{g} = 10^{-1}$, whereas in the right plot $\bar{g} = 1$. See text for details.

hierarchies, c_{Na}, and the dimensionless couplings $g_{(1,2)aa}$ and g_{NNa}. However, even without sticking to particular parameter values, general conclusions can be made by noting that the relative size of the annihilation and decay reaction densities is mainly determined by

$$\frac{\gamma_S}{\gamma_D} \sim \frac{\bar{g}^4 v^2}{M_{N_1}\widetilde{m}_1} \ , \tag{14}$$

where with $\bar{g}$ we refer to any of the couplings entering in the cross section in Eqs. (7)-(9) [4]. For simplicity, in most of our analysis we will assume "universality" of these couplings. Thus, for a given M_{N_1}, the relevance of the scalar-induced RH neutrino scattering will depend on $\widetilde{m}_1$ and $\bar{g}$. A small $\bar{g}$ will lead to a sub-dominant scattering process ($\gamma_S < \gamma_D$) unless $\widetilde{m}_1$ is small as well (the precise values determined by specific parameter choices), while large values of $\bar{g}$ will render the RH neutrino scattering a dominant process up to large values of z. As shown in the following section, this behavior has striking consequences, namely it can either dramatically enhance or suppress the $B - L$ yield.

Although there is no fundamental reason for the different dimensionless couplings to be equal nor for the scalar masses to be well below the RH neutrino mass, it turns out that these simplifying "universality" assumptions capture the main features of the role played by RH neutrino scatterings in seesaw leptogenesis (see discussion in section III C). The generic behavior described above is illustrated in Fig. 2, where for concreteness we have taken the RH neutrino mass to be 10^{10} GeV, and the dimensionless couplings to be 10^{-1} (left panel) and 1 (right panel). So, for example, while a decay controlled by $\widetilde{m}_1 = 0.01$ eV becomes dominant already at $z \sim 1$ when $\bar{g} = 10^{-1}$, (i.e. RH neutrinos will not be able to thermalize by the scatterings), the same decay will be severely swamped by RH neutrino scatterings when $\bar{g} = 1$.

[4] We would like to emphasize that $\bar{g}$ is any of the parameters participating in the scattering cross section, which only involves N_1 (and not $N_{2,3}$). This is because, by assumption (see footnote 3), the dynamics of the problem are fully dictated by the lightest RH neutrino, much lighter than the other two. For this reason, all parameters in Eq.(14) are related only to N_1.

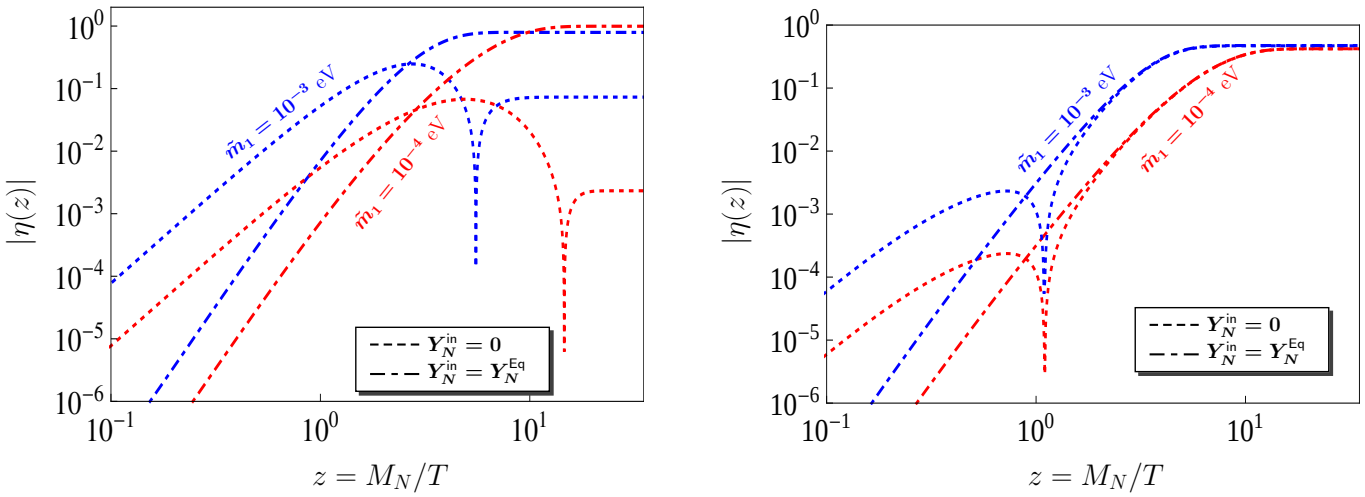

FIG. 3: Efficiency function $\eta(z)$ in Eq. (18) for two representative $\widetilde{m}_1$ values in the weak washout regime. The left panel is the standard case, while the right panel includes the effects of right-handed scatterings with $\bar{g} = 10^{-1}$ and $M_{N_1} = 10^{10}$ GeV. One sees that the $B - L$ asymmetry at the end of the leptogenesis era is independent of the initial RH neutrino distribution.

III. THE BARYON ASYMMETRY FROM LEPTOGENESIS

With the general picture already clear, in this section we will analyze the implications of the scalar-mediated right-handed neutrino scatterings for the generation of the $B-L$ asymmetry. For this aim we need to write suitable kinetic equations with which the $B - L$ asymmetry can be tracked. Depending on the dynamics of the new scalars, these equations can substantially differ from those of the standard case [50, 51].

A. Dynamical features of the $B - L$ asymmetry generation

First note that if the heat bath before the leptogenesis era becomes populated with the new scalars, and their interactions are such that their distributions obey

$$\frac{Y_{S_a}}{Y_{S_a}^{\rm Eq}} \simeq 1 + \theta \qquad \text{with} \qquad \theta \ll 1 \ , \tag{15}$$

then the corresponding kinetic equations take a rather simple form, similar to the kinetic equations found in fermionic triplet leptogenesis scenarios [34, 35, 39]. Note that the new scalars will at least couple via scalar vertices to the standard model Higgs doublet [5]. The thermal bath will then be populated with the new scalars either directly after reheating [32], or through the interactions characterizing the scalar sector in Eq. (5). In this case Eq. (15) will hold provided the scalar interactions are strong enough. Using Eq. (15) we write the system of coupled Boltzmann differential equations at order λ^2 from Eq. (4) as [6]

$$\frac{d}{dz}Y_N = -\frac{1}{\mathsf{s}Hz}\left\{\left(\frac{Y_N}{Y_N^{\rm Eq}} - 1\right)\gamma_D + \left[\left(\frac{Y_N}{Y_N^{\rm Eq}}\right)^2 - 1\right]\gamma_S\right\} \ , \tag{16}$$

[5] Depending on the model the new scalars might also have gauge and/or new Yukawa interactions.
[6] We neglect spectator processes, work in the one-flavor-approximation, and drop order θ terms.

$$\frac{d}{dz}Y_{\Delta_{B-L}} = -\frac{1}{\mathsf{s}Hz}\left[\left(\frac{Y_N}{Y_N^{\rm Eq}}-1\right)\epsilon_N + \frac{Y_{\Delta_{B-L}}}{2\,Y_\ell^{\rm Eq}}\right]\gamma_D \ . \tag{17}$$

Here $Y_X = n_X/\mathsf{s}$ is the number density-to-entropy ratio of species X and s denotes the entropy density. Formal integration of these equations allows one to express the $B-L$ asymmetry in terms of the efficiency η as [52]

$$Y_{\Delta_{B-L}}(z) = Y_N^{\rm Eq}(z\to 0)\,\epsilon_N\,\eta(z)\ , \tag{18}$$

with the final $B-L$ yield $Y_{\Delta_{B-L}}(z\to\infty)$ determined by the particle physics CP asymmetry parameter ϵ_N and the washout dynamics, characterized by the efficiency parameter η defined as $\eta \equiv \eta(z\to\infty)$. Here $Y_N^{\rm Eq}(z\to 0)$ is a normalization factor.

Integrating equations (16) and (17) we now derive the consequences of the new RH neutrino scattering reactions on the generation of the $B-L$ asymmetry. We first consider the weak washout regime, given by the condition $\widetilde{m}_1 \lesssim m_\star$ with $m_\star \simeq 10^{-3}$ eV, entirely determined by cosmological input, see e.g. [27]. We calculate the efficiency for two values of $\widetilde{m}_1 = 10^{-3}, 10^{-4}$ eV assuming two different initial RH neutrino densities: vanishing and equilibrium, and for the parameters fixed as in the left panel in Fig. 2. As seen in the left panel in Fig. 3, in the standard case the $B-L$ yield strongly depends upon the initial RH neutrino abundance, as expected [52]. In contrast, as we have pointed out in the previous section, the presence of the new scattering processes can change that picture drastically provided the scattering reaction rate for $S_a\,S_a \to N_1\,N_1$ is larger than the inverse decay rate at early times (high temperatures). In such case the heat bath will be populated with RH neutrinos through scattering processes rather than by slow inverse decays. This result clearly demonstrates that the presence of the scalar-induced RH neutrino scattering renders the $B-L$ yield independent of assumptions regarding the initial RH neutrino population, involving only ϵ_N, $\tilde{m}_1$, M_{N_1} and $\bar{g}$, see right panel in Fig. 3.

The result in Fig. 3 exhibits an additional feature. In the absence of the scalar-mediated RH neutrino scattering, i.e. if $\gamma_S \ll \gamma_D$ (standard case) and in the weak washout regime, say $\widetilde{m}_1 = 10^{-4}$ eV, and $Y_N^{\rm in} = 0$, one finds that the efficiency at freeze-out is determined by $\eta \sim \widetilde{m}_1/m_\star$ (see left panel in Fig. 3), as expected [50]. However, one sees in the right panel of Fig. 3 that the efficiency is almost maximal for $\widetilde{m}_1 = 10^{-4}$ eV. This enhancement can be traced back to the way in which the thermal bath becomes populated with RH neutrinos at early epochs: regardless of the strength of the scattering process, if at high temperatures (small z's) the condition $\gamma_S > \gamma_D$ is satisfied, then the RH neutrino population becomes dictated by these processes, reaching large values more rapidly than if determined by inverse decays. The overall effect of the RH annihilation reactions can then be "dissected" as follows:

- *Enhancement of the efficiency*: if at early epochs the condition $\gamma_S > \gamma_D$ is satisfied and the scalar-induced RH neutrino scatterings are slow throughout the relevant temperature range, the efficiency is enhanced, readily reaching almost maximal values. This can lead to a dramatic enhancement in the weak washout regime.

- *Suppression of the efficiency*: if at high temperatures the condition $\gamma_S > \gamma_D$ is satisfied, but during a certain period the RH neutrino scattering processes are fast, the efficiency can be strongly suppressed due to the RH neutrino thermalization induced by these reactions.

These effects are illustrated in Fig. 4, for the same parameter choice as in Fig. 2. The case of *efficiency enhancement* (Fig. 4, left) can be understood from Fig. 2, left, as follows. Although $\gamma_S > \gamma_D$ holds at high temperatures even in the strong washout regime, for $\widetilde{m}_1 > 10^{-3}$ eV the inverse decay becomes dominant at lower temperatures. In this case the efficiency matches the standard result, as seen in the left panel of Fig. 4. In contrast, for parameters in the weak washout regime the RH neutrino population is determined by the scalar-induced RH neutrino scatterings, too slow to thermalize the RH neutrino distribution for a long period, thus resulting in an striking enhancement of the efficiency. Turning to the case of *efficiency suppression* (Fig. 4, right) one finds that, due to fast scatterings, RH neutrinos follow a thermal distribution down to significantly low temperatures (large z). Thus, although the number of RH neutrinos

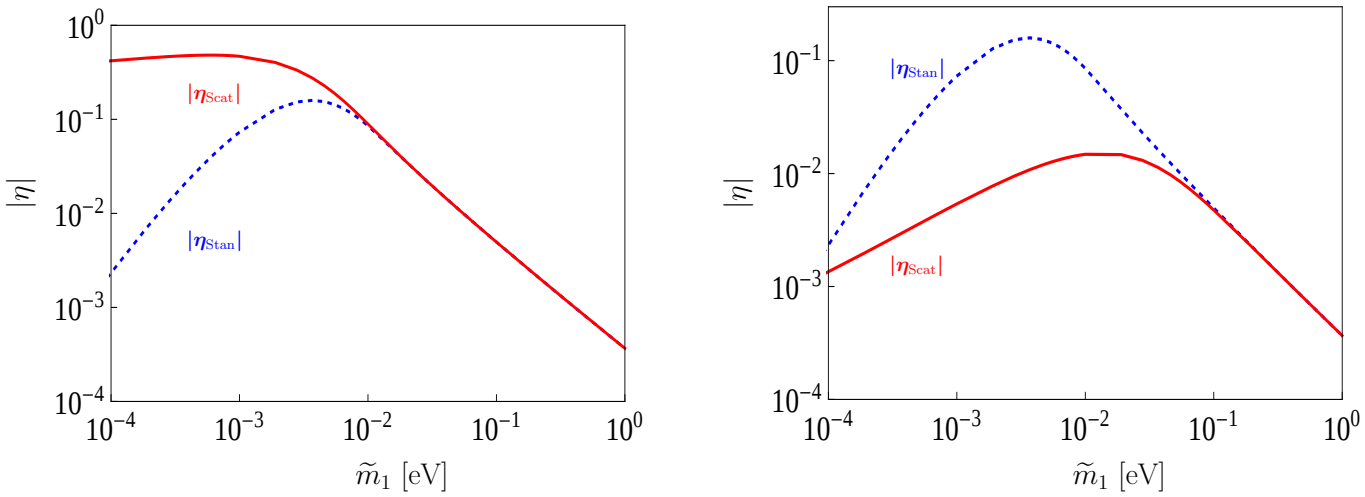

FIG. 4: Efficiency versus $\widetilde{m}_1$ for the scattering parameters fixed as in Fig. 2. The red (solid) curve corresponds to the efficiency obtained when RH neutrino scatterings are included while the blue curve (dotted) to the efficiency in the standard case.

present in the heat bath is large, the overall efficiency is far smaller as a result of RH neutrino thermalization caused by the fast RH scalar-induced neutrino scatterings. Note however that for large enough values of $\widetilde{m}_1$ the generation of the $B-L$ asymmetry proceeds as in the standard case. The reason is again that for values of $\widetilde{m}_1$ deep inside the strong washout regime, the RH neutrino inverse decay is still operative and dominant when the scattering interactions are decoupled.

B. Confronting observation

In the presence of rapid fermion-number violation due to non-perturbative electroweak effects [29], the baryon number of the Universe is obtained from the $B-L$ asymmetry of the Universe generated as a result of the right-handed neutrino decays. Using the standard result [53]

$$Y_{\Delta_B} = (12/37)\, Y_{\Delta_{B-L}}\,, \tag{19}$$

and the experimental value $Y_{\Delta_B} \subset [8.52, 8.98] \times 10^{-11}$ [2, 3] one can derive, from Eq. (18), a lower limit for the efficiency in terms of the CP asymmetry factor ϵ_N

$$\eta \gtrsim \frac{7\times 10^{-8}}{\epsilon_N}\,. \tag{20}$$

One sees that, depending on the CP asymmetry parameter, largely model-dependent, one has a minimum required value for the efficiency in order to generate the correct baryon asymmetry. For example, for the unrealistic case of maximal CP asymmetry [7], $\epsilon_N = 1$, any parameter choice for which the efficiency factor drops below $\sim 7\times 10^{-8}$ will be unacceptable. Thus, for a given strength of the scalar couplings one can determine the allowed $(\widetilde{m}_1, M_{N_1})$ values for which the resulting $B-L$ is acceptable.

We have seen that the presence of the scalar-induced RH neutrino scattering processes can have dramatic consequences in the weak washout regime, either enhancing or suppressing the efficiency depending on the scalar coupling

[7] For strongly hierarchical RH neutrinos, such values are not possible without new contributions to the CP asymmetry [38].

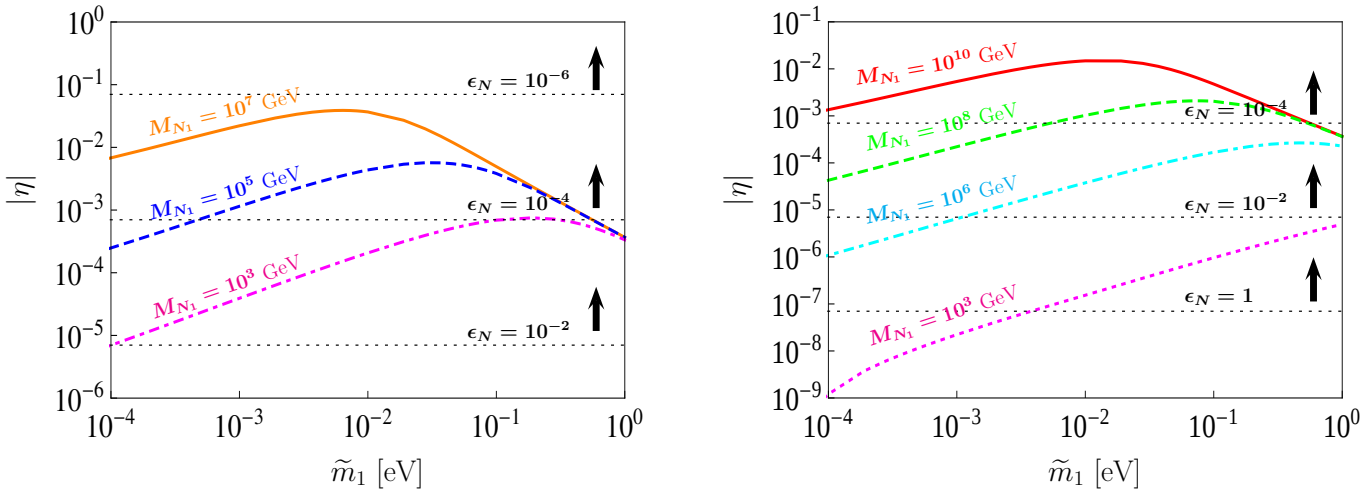

FIG. 5: Efficiency as a function of $\widetilde{m}_1$ for several values of the RH neutrino mass and two different (representative) choices of the "universal" coupling $\bar{g} = 10^{-1}$ left plot while $\bar{g} = 1$ right plot. The horizontal lines indicate the minimum value that, for a given CP asymmetry, the efficiency parameter should have in order for the $B - L$ mechanism to successfully reproduce the measured B asymmetry.

parameter $\bar{g}$. The latter suggests that there should exist parameter choices for which the thermalization, induced by the annihilation process, may be still consistent with the generation of an adequate baryon asymmetry. For example for $M_{N_1} = 10^{10}$ GeV, even maximizing the scattering rate does not necessarily render the $B-L$ asymmetry below the required value (Fig. 4, right plot). In the range where the RH neutrino scattering is effective $\widetilde{m}_1 \subset [10^{-4}, 10^{-1}]$ eV, the smallest value the efficiency has is about 10^{-3}, and therefore according to Eq. (20) a CP asymmetry factor of order 10^{-4} would suffice. This exercise shows that in terms of the RH neutrino mass and scattering cross section (see Eqs. (7)-(9)), one can identify, given certain value for the CP asymmetry, those scenarios for which the efficiency depleting effect becomes "harmless" no matter the parameter choice, and those for which the depleting effect render the $B - L$ asymmetry generation mechanism ineffective.

We illustrate quantitatively the requirements for a successful leptogenesis scenario in Fig. 5, which shows the efficiency for two representative values of the "universal" coupling, $\bar{g} = 10^{-1}$ for the left plot and $\bar{g} = 1$ for the right plot, and different RH neutrino masses. The horizontal dotted lines indicate the minimum required efficiency values, given a fixed CP asymmetry factor, see Eq. (20). Points in the efficiency curves lying below (above) those lines indicate RH neutrino masses for which the leptogenesis mechanism fails (succeeds) in accounting for the baryon asymmetry. From this one can draw several generic conclusions: (i) if the CP asymmetry can be very large ($\epsilon_N \gtrsim 10^{-2}$), the scalar-induced RH neutrino scattering does not place any significant constraint as seen in the left plot; (ii) for the interesting range $\bar{g} \subset [10^{-1}, 1]$, RH neutrinos with masses obeying $M_{N_1} > 10^8$ GeV ($M_{N_1} > 10^{11}$ GeV) can produce an adequate $B - L$ asymmetry provided the CP asymmetry exceeds 10^{-6} and $\bar{g} = 10^{-1}$ ($\bar{g} = 1$). In short, the scalar-induced RH neutrino scattering constraints become most relevant in those scenarios where getting a large CP asymmetry is not viable.

C. Beyond the simplified scenario

Finally, let us justify the usefulness of the simplified scenario with massless spin zero states and universal dimensionless couplings. All our previous numerical results have been obtained in this scenario and thus the question arises as to whether they would be different, at least qualitatively, in more general cases with massive scalars and

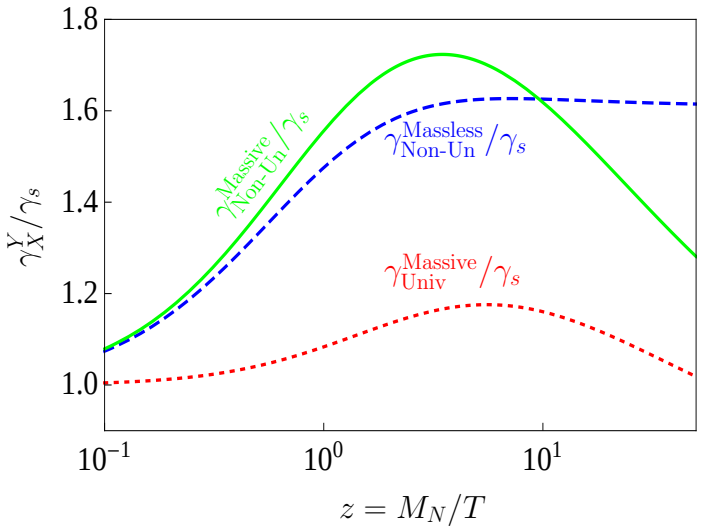

FIG. 6: Ratios of right-handed neutrino scattering reaction densities as a function of $z = M_N/T$ for various scenarios. Solid (green) corresponds to massive scalars ($m_{S_1} = M_{N_1}$) and non-universal couplings; dashed (blue) to massless scalars and non-universal couplings; dotted (red) to massive scalars ($m_{S_1} = M_{N_1}$) and universal couplings. In all cases the normalization is given by the RH neutrino scattering reaction density calculated for massless scalars and universal couplings. See text for details.

arbitrary coupling patterns. Fig. 6 answers this question. It shows the annihilation reaction density as a function of z for several scenarios normalized to the one calculated in the limit of massless scalars ($m_{S_a} \ll M_{N_1}$) and universal couplings ($\bar{g} = 1$). The cases correspond to: massive S_1, its mass fixed as $m_{S_1} = M_{N_1}$, and non-universal couplings $g_{NNa} = 1$ and $g_{abc} = 10^{-1}$ (solid/green curve); massless scalars and non-universal couplings $g_{NNa} = 1$ and $g_{abc} = 10^{-1}$ (dashed/blue curve); massive S_1 and universal couplings (dotted/red curve). This result demonstrates what we already anticipated in Sec. II, namely deviations obtained as a result of "non-universality" and sizeable scalar masses are small, and so do not change the general picture derived by using the simplest scenario. This can be readily understood by inspecting the $N_1 N_1 \leftrightarrow S_a\, S_a$ scattering cross section in Eq. (6). The dominant contributions are the ones given by the t- and u-channel diagrams, as can be seen by comparing their contributions to the total cross section to the s-channel contribution: $\sigma_{t,u}(s)/\sigma_s(s) \sim 2x_N + 4\log(x_N) \gg 1$, where we have assumed universal couplings. The only exception is found for $g_{NNa} \ll g_{abc}$, but in that case the RH neutrino scattering process plays no role in the generation of the $B - L$ asymmetry. Since the t- and u-channel diagrams only depend on the g_{NNa} couplings and are mediated by RH neutrino exchange, the purely scalar couplings and the masses of the spin zero states play a secondary role in the determination of the annihilation reaction density, explaining why the simplified scenario gives a good description.

IV. THE CASE OF SPONTANEOUS LEPTON NUMBER BREAKING

Let us now apply the results derived in the previous sections to the simplest seesaw majoron model discussed in Sec. I [14, 15]. Type-I seesaw majoron leptogenesis has already been partially analyzed in Refs. [37, 54]. We start the analysis by discussing the main features of this scheme.

A. Scalar sector

The extended scalar sector of the model consists of the Higgs doublet, H, and a new $\mathrm{SU(3)_c} \otimes \mathrm{SU(2)_L} \otimes \mathrm{U(1)_Y}$ singlet complex scalar field, σ, carrying lepton number charge $L = -2$. For simplicity we assume CP invariance in the scalar potential. After the electroweak gauge symmetry and lepton number get broken, one gets the following mass terms for the neutral scalars (ρ) and pseudoscalars (κ)

$$V_{\text{quadratic}} \supset \frac{1}{2}\rho_a \left(M_S^2\right)_{ab} \rho_b + \frac{1}{2}\kappa_a \left(M_P^2\right)_{ab} \kappa_b \ , \tag{21}$$

where a sum over the scalar indices $a, b = 1, 2$ has been left implicit. In the basis $\rho = \mathrm{Re}\left(\sigma, \phi^0\right)^T$ and $\kappa = \mathrm{Im}\left(\sigma, \phi^0\right)^T$ the mass matrices M_S^2 and M_P^2 are given by

$$M_S^2 = \begin{pmatrix} \frac{1}{4}\left(6\lambda_\sigma u^2 - 2m_\sigma^2 + \delta v^2\right) & \frac{1}{2}\delta v u \\ \frac{1}{2}\delta v u & \frac{1}{4}\left(\delta u^2 - 2m_H^2 + 6\lambda_H v^2\right) \end{pmatrix} \ , \tag{22}$$

$$M_P^2 = \begin{pmatrix} \frac{1}{4}\left(2\lambda_\sigma u^2 - 2m_\sigma^2 + \delta v^2\right) & 0 \\ 0 & \frac{1}{4}\left(\delta u^2 - 2m_H^2 + 2\lambda_H v^2\right) \end{pmatrix} . \tag{23}$$

The neutral scalar mass matrix M_S^2 becomes diagonal by going to the mass basis $S = (S_1, S_2)^T = R_S^\dagger \rho$, where R_S is a unitary matrix such that $R_S M_S^2 R_S^\dagger = \mathrm{diag}(m_{S_1}^2, m_{S_2}^2)$. After applying the minimization conditions for the scalar potential in Eq. (3), the resulting mass eigenvalues and unitary matrix R_S are found to be

$$m_{S_{1,2}}^2 = \frac{1}{2}\left(\lambda_\sigma u^2 \pm \tilde{u}^2 + \lambda_H v^2\right) \ , \tag{24}$$

$$R_S = \begin{pmatrix} -\frac{\lambda_H v^2 - \tilde{u}^2 - \lambda_\sigma u^2}{\sqrt{\delta^2 u^2 v^2 + (\lambda_H v^2 - \tilde{u}^2 - \lambda_\sigma u^2)^2}} & \frac{\delta u v}{\sqrt{\delta^2 u^2 v^2 + (\lambda_H v^2 - \tilde{u}^2 - \lambda_\sigma u^2)^2}} \\ \frac{-\lambda_H v^2 - \tilde{u}^2 + \lambda_\sigma u^2}{\sqrt{\delta^2 u^2 v^2 + (-\lambda_H v^2 - \tilde{u}^2 + \lambda_\sigma u^2)^2}} & \frac{\delta u v}{\sqrt{\delta^2 u^2 v^2 + (-\lambda_H v^2 - \tilde{u}^2 + \lambda_\sigma u^2)^2}} \end{pmatrix} , \tag{25}$$

where we have defined

$$\tilde{u}^2 = \sqrt{\lambda_\sigma^2 u^4 + u^2 v^2 (\delta^2 - 2\lambda_H \lambda_\sigma) + \lambda_H^2 v^4} \, . \tag{26}$$

In the limit $\delta \ll 1$ (or, similarly, for $v \ll u$) the mixing between the two scalar states becomes negligible. In this scenario S_1 is mainly singlet, with a squared mass $m_{S_1}^2 \simeq \lambda_\sigma u^2$. The other state, with a squared mass $m_{S_2}^2 \equiv m_h^2 \simeq \lambda_H v^2$, is identified as the standard model Higgs boson. On the other hand, the pseudoscalar mass matrix M_P^2 contains two vanishing eigenvalues. After minimizing the scalar potential it simplifies to a 2×2 matrix with vanishing entries. As expected, the spontaneous breaking of lepton number implies the existence of a massless physical Nambu-Goldstone boson, the majoron J, with a pure singlet nature. The other massless pseudoscalar state corresponds to the would-be Goldstone boson that becomes the longitudinal component of the Z boson. We can then make the following identification $P = (P_1, P_2)^T \equiv \left(J, G^0\right)^T$ and $S_3 \equiv P_1$, S_3 being the generic pseudoscalar field introduced in Sec. II.

In order to identify the g_{NNa} and g_{abc} couplings used in Sec. III in terms of the "fundamental" parameters of the model, one must find the corresponding expressions for these couplings, namely [8]

$$g_{NN1} = -\frac{h}{\sqrt{2}} R_S^{11} \ , \tag{27}$$

$$g_{NN2} = -\frac{h}{\sqrt{2}} R_S^{12} \ , \tag{28}$$

[8] In this section we will use a simplified notation in which h actually refers to h_{11}, the element of the h Yukawa matrix that involves two N_1's.

$$\mu_{111} = \frac{1}{2}\left[2u\lambda_\sigma \left(R_S^{11}\right)^3 + \delta u R_S^{11}\left(R_S^{21}\right)^2 + \delta\left(R_S^{11}\right)^2 R_S^{21} v + 2\lambda_H \left(R_S^{21}\right)^3 v\right] , \tag{29}$$

$$\begin{aligned}\mu_{112} = \frac{1}{2}\Big[&u\left(6\lambda_\sigma \left(R_S^{11}\right)^2 R_S^{12} + 2\delta R_S^{11} R_S^{21} R_S^{22} + \delta R_S^{12}\left(R_S^{21}\right)^2\right) \\ &+v\left(\delta\left(R_S^{11}\right)^2 R_S^{22} + 2\delta R_S^{11} R_S^{12} R_S^{21} + 6\lambda_H \left(R_S^{21}\right)^2 R_S^{22}\right)\Big] ,\end{aligned} \tag{30}$$

$$\begin{aligned}\mu_{122} = \frac{1}{2}\Big[&u\left(6\lambda_\sigma R_S^{11}\left(R_S^{12}\right)^2 + \delta R_S^{11}\left(R_S^{22}\right)^2 + 2\delta R_S^{12} R_S^{21} R_S^{22}\right) \\ &+v\left(2\delta R_S^{11} R_S^{12} R_S^{22} + \delta\left(R_S^{12}\right)^2 R_S^{21} + 6\lambda_H R_S^{21}\left(R_S^{22}\right)^2\right)\Big] ,\end{aligned} \tag{31}$$

$$\mu_{222} = \frac{1}{2}\left[2u\lambda_\sigma \left(R_S^{12}\right)^3 + \delta u R_S^{12}\left(R_S^{22}\right)^2 + \delta\left(R_S^{12}\right)^2 R_S^{22} v + 2\lambda_H \left(R_S^{22}\right)^3 v\right] , \tag{32}$$

$$\mu_{133} = \lambda_\sigma u R_S^{11} + \frac{1}{2}\delta v R_S^{21} , \tag{33}$$

$$\mu_{233} = \lambda_\sigma u R_S^{12} + \frac{1}{2}\delta v R_S^{22} . \tag{34}$$

The above relations simplify in the limit in which the singlet-doublet mixing is negligible (given by $\delta \ll 1$ or $v \ll u$). In this case R_S is the 2×2 identity matrix and one finds

$$g_{NN1} = -\frac{h}{\sqrt{2}} , \qquad g_{NN2} = 0 , \tag{35}$$

$$\mu_{111} = \mu_{133} = u\lambda_\sigma , \qquad \mu_{112} = \mu_{233} = \frac{1}{2}v\delta , \tag{36}$$

$$\mu_{122} = \frac{1}{2}u\delta , \qquad \mu_{222} = \lambda_H v . \tag{37}$$

The explicit efficiency calculation presented in Sec. III reveals that the most important parameters can be chosen as the right-handed neutrino mass M_{N_1} and its coupling to the scalars g_{NNa}.

B. The $B - L$ asymmetry in the presence of majorons

We now turn to the interpretation of our results in terms of the relevant majoron model parameters, chosen as the scale of spontaneous lepton number violation u and the Yukawa coupling h. In the left panel in Fig. 7 we show our results for the efficiency in the h-u plane, obtained for a fixed value of $\widetilde{m}_1 = 10^{-3}$ eV, for RH neutrino masses in the range $[5 \cdot 10^3, 10^{10}]$ GeV. On the other hand in the right panel we have focused on RH neutrino masses in the range $M_N < 5$ TeV. These figures can be easily interpreted using Eq. (20). Each efficiency value can be translated into a necessary value for the CP asymmetry, ϵ_N, which allows for an adequate value for the baryon asymmetry of the Universe. For example, the isocurve for which $\eta = 10^{-6}$ requires $\epsilon_N \sim 10^{-3}$. The contour with $\eta = 6.2 \times 10^{-8}$ shown on the right panel is the lower limit of the viable parameter space region, since it requires a maximal CP asymmetry obeying $\epsilon_N \sim 1$. Points below that contour (hatched region) are thus excluded by the measured baryon asymmetry combined with the $B - L$ yield derived from leptogenesis. One sees the trouble in reconciling a sizeable baryon asymmetry generated through leptogenesis within a minimal seesaw majoron scheme. Note that for low right-handed neutrino masses $M_N < 5$ TeV the $2 \leftrightarrow 2$ RH neutrino annihilation processes are fast down to low temperatures (large z). In this case the RH neutrinos are almost thermalized by these scatterings and hence unable to generate a sufficiently large $B-L$ asymmetry before sphaleron decoupling which, for a Higgs mass of about 125 GeV, takes place at about $T \sim 135$ GeV [55, 56]. This means that the electroweak sphaleron processes freeze out before converting the $B - L$ asymmetry into an adequate baryon asymmetry. This effect should be taken into account whenever dealing with a state whose mass is near the electroweak scale and subject to fast reactions, as it might be the case in low-scale leptogenesis models. Implementation of these scenarios require overcoming the upper limit of the CP asymmetry [38], something which can be in principle done by resorting to extended models with additional

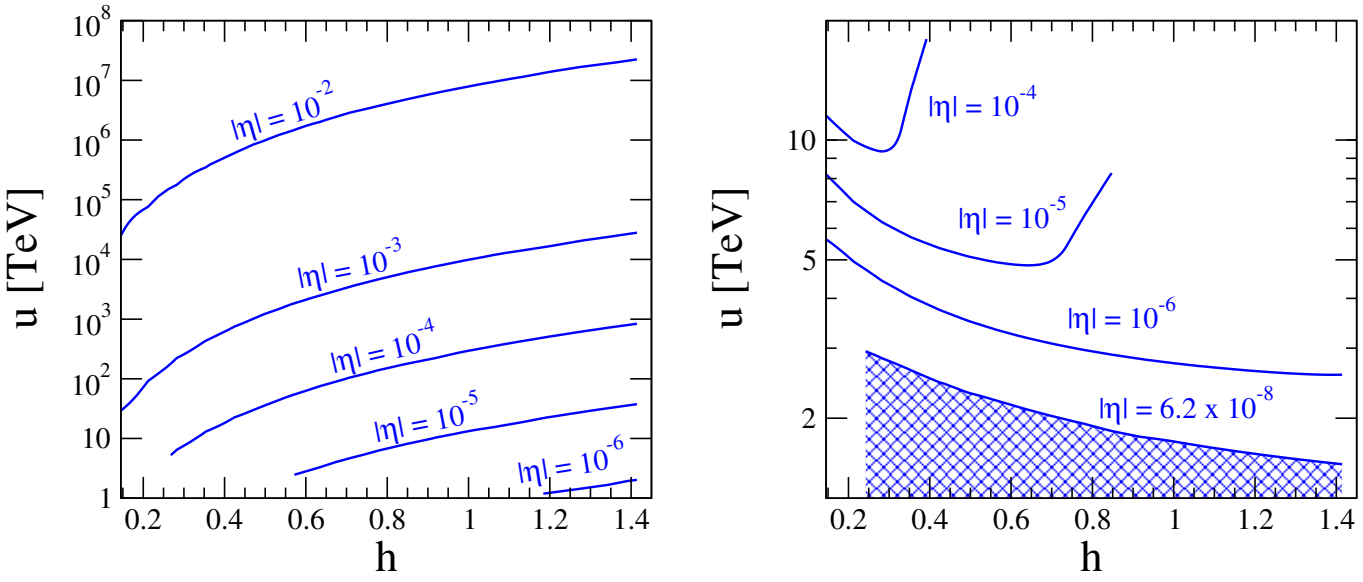

FIG. 7: Efficiency contours in the h-u plane, for a fixed value of $\widetilde{m}_1 = 10^{-3}$ eV. In the left panel we show our results for $M_N > 5$ TeV, while on the right panel we focus on the region with lower right-handed neutrino masses. See text for details.

contributions to the CP asymmetry (not subject to constraints from neutrino masses), see for example [57–59], or by assuring a quasi-degenerate RH neutrino mass spectrum leading to resonant effects [60–62]. These scenarios are beyond the scope of this paper, and so we will not add further details on these specific realizations.

V. CONCLUSIONS

Seesaw schemes with spontaneous lepton number violation generate neutrino mass while potentially addressing other cosmological issues such as the origin of dark matter and inflation. They can also account for the cosmic baryon asymmetry via leptogenesis. These models all require extended Higgs sectors in order to realize an adequate symmetry breaking pattern involving lepton number as well as electroweak breaking. For the simplest case of the standard $\mathrm{SU(2)_L} \otimes \mathrm{U(1)_Y}$ gauge structure and ungauged lepton number, a key feature is the presence of a (pseudo) Nambu-Goldstone boson, the majoron J, associated to the spontaneous breaking of lepton number. Inspired by the attractiveness of such schemes, we have analyzed the effects that the novel right-handed neutrino scalar-mediated annihilation processes ($NN \leftrightarrow S_a S_a$) can have in the generation of the $B-L$ asymmetry. Even in simple realizations, these processes involve many free parameters. However, we have identified the two new parameters which best describe the implications of such scatterings in the generation of the $B-L$ asymmetry. Within our simple description we have shown that scattering processes can change the conventional picture. First note that the heat bath will be populated with the intervening scalars, either produced by reheating or via their couplings with the standard model Higgs. In this case the RH neutrino density in the thermal bath will be determined by the novel scattering reactions rather than by inverse decays. In the parameter regions where these reactions are slow in the relevant temperature range, their presence will tend to enhance the $B-L$ yield, provided the Dirac neutrino Yukawa couplings lie in the weak washout regime. A direct consequence of this is that of the $B-L$ asymmetry will no longer depend upon initial conditions, something inherent to the "standard" picture in the weak washout regime. In contrast, if the new scatterings are fast the RH neutrino distribution will closely follow a thermal distribution. Although such effect will tend to suppress the $B-L$ yield, it need not invalidate the $B-L$ production mechanism, provided the CP-asymmetry is large enough. In any case, a proper treatment of the $B-L$ asymmetry generation mechanism within these schemes requires the

inclusion of RH neutrino annihilations, as long as the relevant couplings are sizeable.

Before closing let us mention that the presence of Goldstone bosons, such as the majoron, if associated to low-scale symmetry breaking, may give rise to other non-standard signatures. For example, it can induce a large standard model Higgs invisible decay mode [63]. The restrictions on the parameter space are determined by the upper limit on the invisible decay width of the Higgs boson. The current upper bound given by the ATLAS collaboration [64] for the invisible decay mode branching ratio is not too stringent, allowing for invisible modes ranging from 10% up to 75%, and thus leaving large fractions of parameter space still open. In the next LHC run a better sensitivity to this mode will be possible. On the other hand, these schemes may also lead to exotic lepton flavor violating decays with majoron emission, such as $\mu \to eJ$ or $\mu \to eJ\gamma$ [65–67]. In any case all these possibilities require low lepton number violation scale, which do not fit within the minimal dynamical leptogenesis schemes considered above. Extended seesaw leptogenesis schemes with right-handed neutrino scatterings lie outside the scope of this paper.

VI. ACKNOWLEDGMENTS

DAS and AV would like to thank Juan Racker for useful comments. This work was supported by MINECO grants FPA2011-22975, MULTIDARK Consolider CSD2009-00064. DAS is supported by a "Chargé de Recherches" contract funded by the Belgian FNRS agency. AV is partially supported by the EXPL/FIS-NUC/0460/2013 project financed by the Portuguese FCT.

[1] D. Forero, M. Tortola and J. W. F. Valle, Phys.Rev. **D86**, 073012 (2012), [arXiv:1205.4018]; for review with a comprehensive set of references see M. Maltoni, T. Schwetz, M. Tortola and J. Valle, New J.Phys. **6**, 122 (2004), [hep-ph/0405172].
[2] WMAP, G. Hinshaw et al., Astrophys.J.Suppl. **208**, 19 (2013), [1212.5226].
[3] Planck Collaboration, P. Ade et al., 1303.5076.
[4] P. Minkowski, Phys. Lett. **B67**, 421 (1977).
[5] M. Gell-Mann, P. Ramond and R. Slansky, (1979), Print-80-0576 (CERN).
[6] T. Yanagida, (KEK lectures, 1979), ed. O. Sawada and A. Sugamoto (KEK, 1979).
[7] G. Lazarides, Q. Shafi and C. Wetterich, Nucl. Phys. **B181**, 287 (1981).
[8] R. N. Mohapatra and G. Senjanovic, Phys. Rev. Lett. **44**, 91 (1980).
[9] J. Schechter and J. W. F. Valle, Phys. Rev. **D22**, 2227 (1980).
[10] R. N. Mohapatra and J. W. F. Valle, Phys. Rev. **D34**, 1642 (1986).
[11] E. Akhmedov et al., Phys. Lett. **B368**, 270 (1996), [hep-ph/9507275].
[12] E. Akhmedov et al., Phys. Rev. **D53**, 2752 (1996), [hep-ph/9509255].
[13] M. Malinsky, J. C. Romao and J. W. F. Valle, Phys. Rev. Lett. **95**, 161801 (2005).
[14] Y. Chikashige, R. N. Mohapatra and R. D. Peccei, Phys. Lett. **B98**, 265 (1981).
[15] J. Schechter and J. W. F. Valle, Phys. Rev. **D25**, 774 (1982).
[16] G. B. Gelmini and J. W. F. Valle, Phys. Lett. **B142**, 181 (1984).
[17] M. C. Gonzalez-Garcia and J. W. F. Valle, Phys. Lett. **B216**, 360 (1989).
[18] R. Kallosh, A. D. Linde, D. A. Linde and L. Susskind, Phys. Rev. **D52**, 912 (1995), [hep-th/9502069].
[19] V. Berezinsky and J. W. F. Valle, Phys. Lett. **B318**, 360 (1993), [hep-ph/9309214].
[20] M. Lattanzi and J. W. F. Valle, Phys. Rev. Lett. **99**, 121301 (2007), [arXiv:0705.2406 [astro-ph]].
[21] M. Lattanzi et al., Phys.Rev. **D88**, 063528 (2013), [1303.4685].
[22] F. S. Queiroz and K. Sinha, 1404.1400.
[23] S. M. Boucenna, S. Morisi, Q. Shafi and J. W. F. Valle, 1404.3198.
[24] T. Higaki, R. Kitano and R. Sato, 1405.0013.
[25] BICEP2 Collaboration, P. Ade et al., 1403.3985.

[26] M. Fukugita and T. Yanagida, Phys. Lett. **B174**, 45 (1986).

[27] S. Davidson, E. Nardi and Y. Nir, Phys.Rept. **466**, 105 (2008), [0802.2962].

[28] C. S. Fong, E. Nardi and A. Riotto, Adv.High Energy Phys. **2012**, 158303 (2012), [1301.3062].

[29] V. A. Kuzmin, V. A. Rubakov and M. E. Shaposhnikov, Phys. Lett. **B155**, 36 (1985).

[30] J. W. F. Valle, Phys. Lett. **B196**, 157 (1987).

[31] J. C. Pati and A. Salam, Phys. Rev. **D10**, 275 (1974).

[32] D. J. Chung, E. W. Kolb and A. Riotto, Phys.Rev. **D60**, 063504 (1999), [hep-ph/9809453].

[33] T. Hambye, M. Raidal and A. Strumia, Phys. Lett. **B632**, 667 (2006), [hep-ph/0510008].

[34] T. Hambye, New J.Phys. **14**, 125014 (2012), [1212.2888].

[35] D. Aristizabal Sierra, J. F. Kamenik and M. Nemevsek, JHEP **1010**, 036 (2010), [1007.1907].

[36] D. Aristizabal Sierra, M. Dhen and T. Hambye, 1401.4347.

[37] P.-H. Gu and U. Sarkar, Eur.Phys.J. **C71**, 1560 (2011), [0909.5468].

[38] S. Davidson and A. Ibarra, Phys. Lett. **B535**, 25 (2002), [hep-ph/0202239].

[39] T. Hambye, Y. Lin, A. Notari, M. Papucci and A. Strumia, Nucl.Phys. **B695**, 169 (2004), [hep-ph/0312203].

[40] D. Aristizabal Sierra, F. Bazzocchi and I. de Medeiros Varzielas, Nucl.Phys. **B858**, 196 (2012), [1112.1843].

[41] N. Cosme, JHEP **0408** 027 (2004), [hep-ph/0403209].

[42] J.-M. Frere, T. Hambye and G. Vertongen, JHEP **0901**, 051 (2009), [0806.0841].

[43] S. Blanchet, P. S. B. Dev and R. N. Mohapatra, Phys. Rev. D **82**, 115025 (2010) [arXiv:1010.1471 [hep-ph]].

[44] M. Plumacher, Z. Phys. C **74** 549 (1997), [hep-ph/9604229].

[45] J. Racker and E. Roulet, JHEP **0903** 065 (2009), [0812.4285].

[46] S. Blanchet, Z. Chacko, S. S. Granor and R. N. Mohapatra, Phys. Rev. D **82**, 076008 (2010) [arXiv:0904.2174 [hep-ph]].

[47] W. Buchmuller, V. Domcke and K. Schmitz, Nucl. Phys. B **862**, 587 (2012) [arXiv:1202.6679 [hep-ph]].

[48] J. Schechter and J. W. F. Valle, Phys. Rev. **D24**, 1883 (1981), Err. D25, 283 (1982).

[49] L. Wolfenstein, Phys. Lett. **B107**, 77 (1981).

[50] G. F. Giudice, A. Notari, M. Raidal, A. Riotto and A. Strumia, Nucl. Phys. **B685**, 89 (2004), [hep-ph/0310123].

[51] E. Nardi, J. Racker and E. Roulet, JHEP **0709**, 090 (2007), [0707.0378].

[52] R. Barbieri, P. Creminelli, A. Strumia and N. Tetradis, Nucl. Phys. **B575**, 61 (2000), [hep-ph/9911315].

[53] J. A. Harvey and M. S. Turner, Phys. Rev. **D42**, 3344 (1990).

[54] A. Pilaftsis, Phys.Rev. **D78**, 013008 (2008), [0805.1677].

[55] A. Strumia, Nucl.Phys. **B809**, 308 (2009), [0806.1630].

[56] M. D'Onofrio, K. Rummukainen and A. Tranberg, 1404.3565.

[57] D. Aristizabal Sierra, M. Losada and E. Nardi, Phys.Lett. **B659**, 328 (2008), [0705.1489].

[58] C. S. Fong, M. Gonzalez-Garcia, E. Nardi and E. Peinado, JHEP **1308**, 104 (2013), [1305.6312].

[59] D. Aristizabal Sierra, C. S. Fong, E. Nardi and E. Peinado, JCAP **1402**, 013 (2014), [1309.4770].

[60] M. Flanz, E. A. Paschos, U. Sarkar and J. Weiss, Phys.Lett. **B389**, 693 (1996), [hep-ph/9607310].

[61] L. Covi and E. Roulet, Phys.Lett. **B399**, 113 (1997), [hep-ph/9611425].

[62] A. Pilaftsis, Phys.Rev. **D56**, 5431 (1997), [hep-ph/9707235].

[63] A. S. Joshipura and J. W. F. Valle, Nucl. Phys. **B397**, 105 (1993).

[64] ATLAS Collaboration, G. Aad et al., 1402.3244.

[65] J. C. Romao, N. Rius and J. W. F. Valle, Nucl. Phys. **B363**, 369 (1991).

[66] M. Hirsch, A. Vicente, J. Meyer and W. Porod, Phys.Rev. **D79**, 055023 (2009), [0902.0525].

[67] X. Garcia i Tormo, D. Bryman, A. Czarnecki and M. Dowling, Phys.Rev. **D84**, 113010 (2011), [1110.2874].